Nanotheranostics

International Edition: DOI: 10.1002/anie.201504536
German Edition: DOI: 10.1002/ange.201504536

X-ray Radiation-Controlled NO-Release for On-Demand Depth-Independent Hypoxic Radiosensitization

Wenpei Fan, Wenbo Bu, Zhen Zhang, Bo Shen, Hui Zhang, Qianjun He, Dalong Ni, Zhaowen Cui, Kuaile Zhao, Jiwen Bu, Jiulin Du, Jianan Liu, and Jianlin Shi**

Abstract: *Multifunctional stimuli-responsive nanotheranostic systems are highly desirable for realizing simultaneous biomedical imaging and on-demand therapy with minimized adverse effects. Herein, we present the construction of an intelligent X-ray-controlled NO-releasing upconversion nanotheranostic system (termed as PEG-USMSs-SNO) by engineering UCNPs with S-nitrosothiol (R-SNO)-grafted mesoporous silica. The PEG-USMSs-SNO is designed to respond sensitively to X-ray radiation for breaking down the S–N bond of SNO to release NO, which leads to X-ray dose-controlled NO release for on-demand hypoxic radiosensitization besides upconversion luminescent imaging through UCNPs in vitro and in vivo. Thanks to the high live-body permeability of X-ray, our developed PEG-USMSs-SNO may provide a new technique for achieving depth-independent controlled NO release and positioned radiotherapy enhancement against deep-seated solid tumors.*

It is well known that successful cancer chemotherapy relies on the design of advanced drug delivery systems (DDSs) with the high drug loading and effective tumor targeting advantages.[1] Of particular interest is to develop "intelligent" DDSs for stimuli-responsive drug release and on-demand therapy of cancer.[2] Among the various internal/external stimuli, pH and light have been widely used because of their convenience of operation.[3] However, the variation of pH in different tumors makes the on-demand drug release uncontrollable in terms of applicability,[4] while light suffers from limited tissue penetration and fails to reach the deep-seated tumors.[5] Therefore, the exploration of more efficient controlled release technology free from endogenous difference/limited penetration may be highly attractive to the development of intelligent DDSs.

As a non-invasive exogenous stimulus, high-energy X-ray radiation may be potentially used to trigger drug release both spatially and temporally without any additives.[6] Compared with pH/light, X-ray is expected to demonstrate the following superior advantages in controlling drug release. Firstly, by aid of precise positioning, the highly penetrating X-ray[7] can force the drug release exclusively on a fixed deep-seated lesion area.[8] Secondly, on-demand drug release can be realized by only changing the X-ray radiation dose and duration.[9] Finally, the combination of chemotherapy and radiotherapy can be achieved to enhance the treatment efficacy.[10] Meanwhile, stimuli-responsive DDSs can be further functionalized with diagnostic properties.[11] Upconversion luminescent (UCL) imaging based on upconversion nanoparticles (UCNPs) has attracted extensive attentions because it can offer visual observation of the drug delivery/release process in vitro and in vivo.[12] Moreover, UCNPs enables to provide a multifunctional platform for multi-modal imaging (e.g., UCL/PET/MRI, etc) from the cellular scale to whole-body evaluation with high spatial resolution/detection sensitivity.[13] Taken together, it is of great importance to design a novel class of stimuli-responsive nanotheranostic systems that enable the controlled drug release by X-ray radiation along with non-invasive tracking/monitoring by UCNPs.

Herein, an intelligent stimuli-responsive upconversion nanotheranostic system has been successfully constructed for X-ray-controlled NO release and UCL imaging (Figure 1a). NO has been widely recognized as a "star" biological molecule involved in a variety of physiological processes.[14] Unlike drugs, NO is biologically safe and causes negligible toxicity to normal organs. More importantly, NO in relatively high concentrations can serve as an effective hypoxic radiosensitizer for enhanced radiotherapy efficacy.[15] Therefore, the controlled NO release by X-ray can selectively increase the NO concentrations in tumors for radiosensitization. Moreover, on-demand depth-independent hypoxic radiosensitization can be also realized by simply manipulating the appropriate X-ray dose.

By the aid of nanochemistry, the X-ray-controlled NO-releasing upconversion nanotheranostics were successfully constructed on a synthesized UCNP/silica structure (Figure S1a in the Supporting Information), followed by the modification using biocompatible PEG and NO donor (SNO). Firstly, monodisperse $NaYF_4$:Yb/Er nanoparticles (UCNPs) with uniform spherical morphology (Figure S1b) were prepared, which could emit green and red luminescence

[*] Dr. W. Fan, Prof. W. Bu, Dr. Q. He, Dr. D. Ni, Dr. Z. Cui, Dr. J. Liu, Prof. J. Shi
State Key Laboratory of High Performance Ceramics and Superfine Microstructures, Shanghai Institute of Ceramics, Chinese Academy of Sciences, Shanghai, 200050 (P.R. China)
E-mail: wbbu@mail.sic.ac.cn
jlshi@mail.sic.ac.cn
Prof. Z. Zhang, H. Zhang, Dr. K. Zhao
Department of Radiology, Shanghai Cancer Hospital
Fudan University, Shanghai, 200032 (P.R. China)
Dr. B. Shen
Institute of Radiation Medicine
Fudan University, Shanghai, 200032 (P.R. China)
Dr. J. Bu, Prof. J. Du
State Key Laboratory of Neuroscience, Institute of Neuroscience, Shanghai Institutes for Biological Sciences, Chinese Academy of Sciences, Shanghai, 200031 (P.R. China)

Supporting information for this article is available on the WWW under http://dx.doi.org/10.1002/anie.201504536.

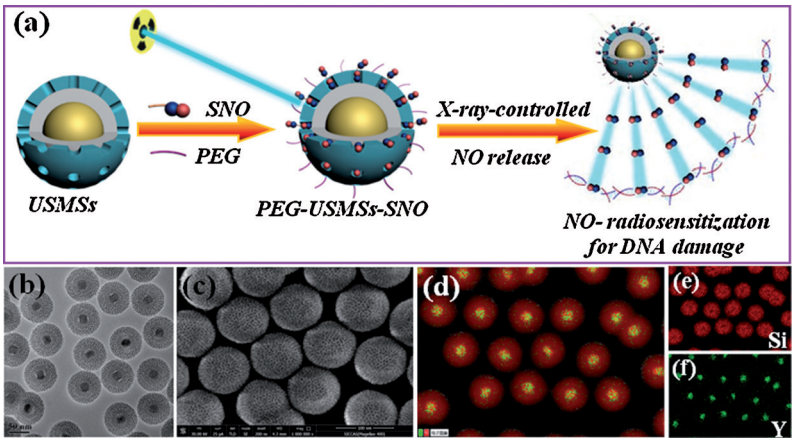

Figure 1. a) Construction of PEG-USMSs-SNO for X-ray-controlled NO release. b) TEM and c) SEM images of USMSs. d–f) The corresponding element mapping of USMSs: e) Si; f) Y; d) mergence of Si and Y.

(Figure S2) upon NIR light ($\lambda = 980$ nm) excitation. Then in order to transfer the synthesized hydrophobic UCNPs to water phase, a dense silica shell was coated on UCNPs (denoted as UCNPs@SiO_2, Figure S1c). Subsequently, a mesoporous silica shell was deposited on UCNPs@SiO_2 (denoted as USMSs, Figure 1b,d and Figure S1d). USMSs possess a relatively high surface area of 369.92 $m^2 g^{-1}$ and pore size centered at 3.2 nm (Figure S3), and the mesoporous channels can be clearly seen from the surface of USMSs (Figure 1c). Next, USMSs were modified with PEG-silane (denoted as PEG-USMSs), then reacted with MPTES to introduce -SH groups, and finally reacted with *tert*-butyl nitrite to yield the product PEG-USMSs-SNO. The FTIR spectrum of PEG-USMSs-SNO (Figure S4) shows the emergence of two new characteristic peaks of -S-N= and -N=O at 764 and 1505 cm^{-1}, respectively, and the UV/Vis spectrum (Figure S5) demonstrates the characteristic absorption of SNO in the range of 330–360 nm ($n_o \rightarrow \pi^*$), both of which confirm the successful conjugation of -SNO groups onto PEG-USMSs.[16] Meanwhile, PEG-USMSs-SNO have a well-defined hydrated particle size distribution centered at 137.7 nm (Figure S6), which indicates their relatively high dispersity/stability.

It has been reported that heat, light and certain metal ions (e.g., Cu^+, Hg^{2+}, etc) can induce/catalyze the homolytic cleavage of S–N bond of SNO to release NO molecules.[14b] However, these stimuli all suffer from intrinsic drawbacks or external influence. As we know, high-energy X-ray radiation is able to break down some low-energy bonds, such as disulfide bond (S–S, 240 kJ mol^{-1}), diselenide bond (Se–Se, 172 kJ mol^{-1}), and has been used to decompose the diselenide/disulfide-containing block polymers for drug release.[6a,9] Considering that the S–N bond energy in the -SNO group (about 150 kJ mol^{-1}) is relatively lower than Se–Se bond energy, we speculated whether S–N bond can be damaged for NO release by X-ray radiation, which will be investigated in the following experiments.

The NO release was quantitatively measured using a typical Griess assay.[17] As shown in Figure 2c, although PEG-USMSs-SNO could spontaneously release a few NO molecules in deionized water, X-ray radiation is certainly able to accelerate the NO release from PEG-USMSs-SNO, and the released NO concentration is gradually increased at elevated X-ray dose. By contrast, there is no NO generation from pure deionized water and PEG-USMSs when exposed to varied doses of X-ray radiation (Figure 2a,b), which indicates that NO does release from the cleavage of S–N bond in PEG-USMSs-SNO. More importantly, NO could be quickly released from PEG-USMSs-SNO, and the maximum release (detailed NO releasing percentage shown in Figure S7) was achieved in 7 h of post-irradiation, though the elevated X-ray dose to 20 Gy may continuously promote NO release beyond 7 h (Figure 2d). This X-ray dose-controlled NO release profile can be understood by the radiation chemistry theory. X-ray can induce the radiolysis of water

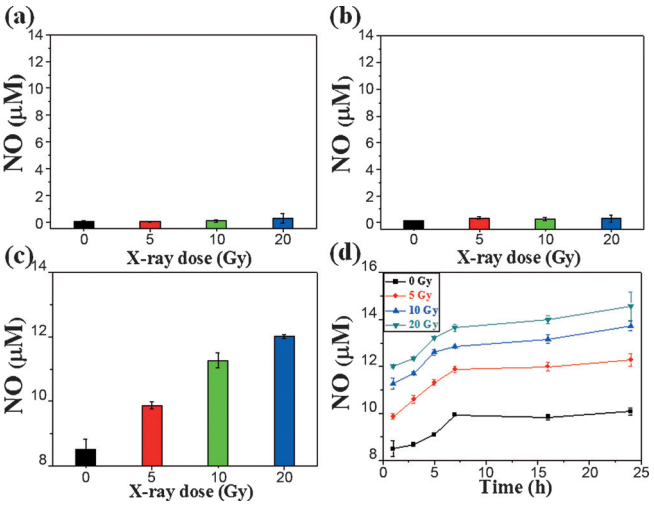

Figure 2. a–c) Quantitative evaluation of immediate NO release from a) deionized water, b) PEG-USMSs, and c) PEG-USMSs-SNO in 1 h after exposure to different doses of X-ray radiation. d) Cumulative NO release from PEG-USMSs-SNO during 24 h after exposure to different doses of X-ray radiation.

into large amounts of multiple ROS, and the -SNO group may undergo a structural variation after interaction with ROS, thus resulting in the cleavage of S–N bond for NO release. As the generated ROS concentrations are proportional to X-ray doses (Figure S8),[9,18] the released NO amount really relies on the generated ROS concentration, which is finally determined by the imposed X-ray dose.

The bio-safety and cytomembrane-permeability are the two critical aspects concerning all drug vehicles, which should be firstly tested. Both non-cancer L929 cells and normal HeLa (denoted as nl-HeLa) cancer cells demonstrate viabilities of about 90% (Figures S9 and S10) after co-incubation with up to 500 μg mL^{-1} PEG-USMSs and PEG-USMSs-SNO in a normoxic atmosphere of 21% O_2/5% CO_2/74% N_2, thus confirming their little cytotocxicity and good biocompatibility. Besides, the green and red luminescence emitted by the

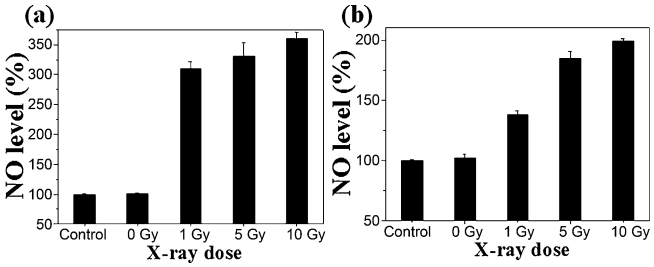

Figure 3. Flow cytometry analysis for NO release in a) nl-HeLa cells and b) hc-HeLa cells after treated with PEG-USMSs-SNO upon different doses of X-ray irradiation. The untreated cells were used as the control.

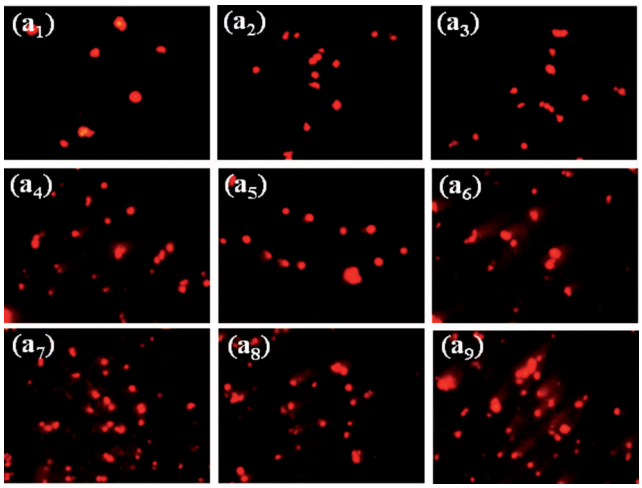

Figure 4. Comet assays for the direct observation of DNA damage of nl-HeLa cells subjected to the following different treatments: a_1) Control; a_2) PEG-USMSs; a_3) PEG-USMSs-SNO; a_4) RT (5 Gy); a_5) PEG-USMSs + RT (5 Gy); a_6) PEG-USMSs-SNO + RT (5 Gy); a_7) RT (10 Gy); a_8) PEG-USMSs + RT (10 Gy); a_9) PEG-USMSs-SNO + RT (10 Gy).

UCNP core appears surrounding the blue nucleus (Figure S11), which indicates that both PEG-USMSs and PEG-USMSs-SNO can penetrate the cell membrane and reach the cytoplasm. Herein, a fluorogenic probe for NO, 3-amino-4-aminomethyl-2′,7′-difluorescein diacetate (DAF-FM DA) was used to track the intracellular NO. As seen from the quantitative result (Figure 3a) by flow cytometry analysis, although NO can be hardly generated in the non-treated (control) and only PEG-USMSs-SNO-treated nl-HeLa cells, more and more NO is produced in nl-HeLa cells treated with both PEG-USMSs-SNO and X-ray radiation, as also evidenced by the corresponding CLSM images in Figure S12, which confirms that X-ray is able to elicit intracellular NO release from PEG-USMSs-SNO. Besides, the NO release in nl-HeLa cells can be well controlled by varying the X-ray doses.

As we know, NO can serve as an effective radiosensitizer to promote tumor cells' apoptosis/necrosis induced by X-ray radiation. As shown by the annexin V-FITC/PI staining results in Figure S13, the combination of PEG-USMSs and radiotherapy (denoted as PEG-USMSs + RT) causes more cells' death than only RT because of the contributions of the high-Z atoms (Y, Yb) in the UCNP core to radiosensitization based on the Compton scattering effects. Much more remarkable apoptosis and necrosis are found in the nl-HeLa cells treated with PEG-USMSs-SNO + RT, which should be attributed to the significant radiation enhancement effects by the released NO.[15] Besides, NO can generate oxidative and nitrosative stress, inhibit mitochondrial respiration, initate inflammation and impair cellular functions, which all contribute to cell apoptosis induction.[14a,b] Certainly, the elevated X-ray dose can trigger larger amount of NO release for further improved radiotherapeutic effects, as evidenced by the higher cells' death rate by PEG-USMSs-SNO + RT (10 Gy) than PEG-USMSs-SNO + RT (5 Gy).

Besides, NO can fix the X-ray-induced DNA damage and inhibit the DNA repair to enhance the radiotherapy efficacy,[15c] which is evaluated by the following comet assay. Only nuclei of their DNA being largely damaged will appear with long stain tails in the comet images. As shown in Figure 4, there emerges negligible stain tail in the nl-HeLa cells treated with PEG-USMSs, PEG-USMSs-SNO, RT or PEG-USMSs + RT, indicating little DNA damages caused by these treatments. However, PEG-USMSs-SNO + RT clearly gives rise to apparently visible long stain tails, implying more significant DNA damages, which may account for the more remarkable cells' apoptosis/necrosis and stronger radiosensitizing effects by the released NO.

Tumor hypoxia is one of the most difficult issues in cancer therapy, so the effect of hypoxic microenvironment on the intracellular X-ray-responsive NO release and radiotherapy efficacy should be carefully studied. After incubation in a hypoxic atmosphere of 2 % O_2/5 % CO_2/93 % N_2 for 24 h, nl-HeLa cells could turn into hypoxic HeLa (denoted as hc-HeLa) cells. Similar to the above nl-HeLa cells, PEG-USMSs and PEG-USMSs-SNO have little cytotoxicity to hc-HeLa cells (Figure S14) and can also be uptaken into the cytoplasm of hc-HeLa cells (Figure S15). In spite of the strong hypoxia, encouragingly, X-ray radiation can still break down the S–N bond and trigger the NO release in hc-HeLa cells by regulating X-ray doses (Figure 3b), though the NO generation are indeed suppressed to varied extents (Figure S16). For example, compared to the control, there is about once enhancement in NO release in hc-HeLa cells treated with PEG-USMSs-SNO + RT (10 Gy) (Figure 3b), which is lower than the twice enhancement in NO release in nl-HeLa cells treated with PEG-USMSs-SNO + RT (1 Gy) (Figure 3a). The slower X-ray-responsive NO release in hc-HeLa cells than in nl-HeLa cells should be attributed to the absence of oxygen that greatly inhibits the ROS generation (Figure S17). As oxygen plays an important role in the radiolysis of water into ROS, the hypoxic atmosphere has led to the decreased ROS concentration under the X-ray-irradiation, and consequently the slower NO release.

Fortunately, though having low efficiency of X-ray-triggered NO release in the hypoxic environment, NO can still enhance the hypoxic tumor responsiveness to X-ray radiation, as reported by De Ridder, et al.[15c] Moreover, NO can diffuse and penetrate freely through hypoxic cells, and

elicit so-called "bystander effect",[15a] which will lead to the overall improvement of radiation enhancement effects. As shown in Figure S18, neither RT nor PEG-USMSs + RT could induce significant hc-HeLa cells' death due to the hypoxic radioresistance. Fortunately, PEG-USMSs-SNO + RT can cause remarkable hc-HeLa cells' apoptosis/necrosis, which confirms that the released NO can stimulate the hypoxic radiosensitization and substantially improve the radiotherapeutic effects on killing massive hypoxic cancerous cells. So our designed PEG-USMSs-SNO could achieve the X-ray dose-controlled NO release and elicit dose-dependent radiotherapeutic effects in normoxic and hypoxic cancerous cells, which encouraged us to perform the in vivo experiments to show the future practicability of PEG-USMSs-SNO.

Due to its optical transparency, zebrafish was chosen as an in vivo model to monitor the X-ray-responsive NO release by CLSM imaging (Figure 5a). After microinjection of PEG-USMSs-SNO into the brain of zebrafish larvae, there appear

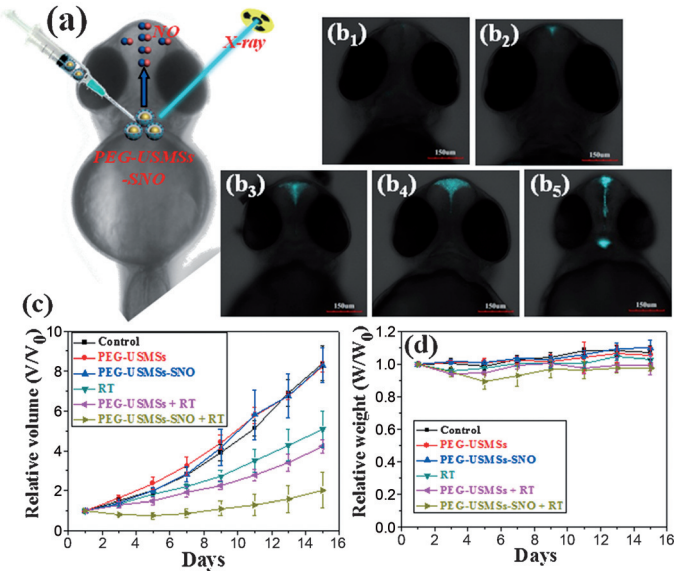

Figure 5. a) X-ray-triggered NO release from PEG-USMSs-SNO in zebrafish larvae. b) CLSM images of NO release in living zebrafish larvae with brain ventricle microinjection of PEG-USMSs-SNO upon exposure to different doses of X-ray radiation: b_1) 0 Gy, b_2) 1 Gy, b_3) 3 Gy, b_4) 5 Gy, b_5) 10 Gy. c) Relative tumor growth curve and d) weight change curve of $4T_1$ tumor-bearing mice over half a month after different treatments.

visible green/red luminescence signals emitted by the UCNP core (Figure S19) but no apparent blue luminescence signal of NO without X-ray irradiation. Remarkably, more and more NO is released upon the increasing doses of X-ray radiation, as evidenced by the gradually intensified blue luminescence signal of NO in the larval brain (Figure 5b). These results unambiguously confirm that PEG-USMSs-SNO can be also used for in vivo X-ray dose-controlled NO release.

Then we further investigated the NO-radiosensitizing effects on treating $4T_1$ solid tumors. In order to maximize the therapeutic effects, the intratumoral injection was conducted to make almost all the injected PEG-USMSs-SNO retained in the tumor (Figure S20).[19] As seen from Figure 5c, both RT and PEG-USMSs + RT only produce limited inhibitory effects on $4T_1$ tumor growth due to the resistance of the interior hypoxic regions to X-ray radiation. Fortunately, PEG-USMSs-SNO + RT can result in the much significant tumor growth delay (Figure S21), which should be attributed to the remarkable radiation enhancement effects by the NO-radiosensitization. In half a month of therapy, the treatment of PEG-USMSs-SNO + RT demonstrates much higher anticancer efficacy and also causes more significant tumor cells' apoptosis/necrosis than other treatments (Figure S22), which further confirms the substantially enhanced NO-sensitized radiotherapy efficacy against cancer in vivo. Finally, neither obvious weight fluctuation (Figure 5d) nor noticeable abnormality in the major organs (Figure S23) has been found, which indicates that PEG-USMSs-SNO are biologically safe and cause little side effects.[10b,20]

In this study, we present the first example of constructing X-ray-controlled NO-releasing upconversion nanotheranostics (PEG-USMSs-SNO) for simultaneous UCL imaging and NO-sensitized radiotherapy of hypoxic cancer. On the basis of S–N bond cleavage upon X-ray irradiation, X-ray-triggered NO release can be achieved without depth dependence, which overcomes the two major barriers (endogenous difference and limited penetration). The in vitro and in vivo results show that PEG-USMSs-SNO can achieve X-ray dose-controlled NO release not only in normoxic/hypoxic cells but also in living zebrafish. Moreover, the released NO demonstrates much stronger radiation enhancement effects on killing hypoxic cancerous cells and inhibiting the solid tumor growth. Finally, our developed PEG-USMSs-SNO may open up new possibilities for the UCL imaging guided on-demand therapy of numbers of deep-seated malignant tumors with much mitigated side effects.

Acknowledgements

This work has been financially supported by the National Natural Science Foundation of China (Grant No. 51372260, 51132009, 21172043, 51102259) and the Opening Project of State Key Laboratory of High Performance Ceramics and Superfine Microstructure (SKL201410SIC).

Keywords: hypoxic radiosensitization · luminescent imaging · NO release · on-demand therapy · X-ray radiation

How to cite: *Angew. Chem. Int. Ed.* **2015**, *54*, 14026–14030
Angew. Chem. **2015**, *127*, 14232–14236

[1] a) L. Palanikumar, E. S. Choi, J. Y. Cheon, S. H. Joo, J.-H. Ryu, *Adv. Funct. Mater.* **2015**, *25*, 957–965; b) F. Gao, L. Li, C. Fu, L. Nie, D. Chen, F. Tang, *Adv. Mater.* **2013**, *25*, 5508–5513.

[2] a) Y. Chen, P. Xu, Z. Shu, M. Wu, L. Wang, S. Zhang, Y. Zheng, H. Chen, J. Wang, Y. Li, J. Shi, *Adv. Funct. Mater.* **2014**, *24*, 4386–4396; b) A. P. Blum, J. K. Kammeyer, A. M. Rush, C. E. Callmann, M. E. Hahn, N. C. Gianneschi, *J. Am. Chem. Soc.* **2015**, *137*, 2140–2154.

[3] a) Y. Chen, H. Chen, S. Zhang, F. Chen, S. Sun, Q. He, M. Ma, X. Wang, H. Wu, L. Zhang, L. Zhang, J. Shi, *Biomaterials* **2012**, *33*, 2388 – 2398; b) J. Liu, W. Bu, L. Pan, J. Shi, *Angew. Chem. Int. Ed.* **2013**, *52*, 4375 – 4379; *Angew. Chem.* **2013**, *125*, 4471 – 4475.
[4] A. Bansal, Y. Zhang, *Acc. Chem. Res.* **2014**, *47*, 3052 – 3060.
[5] a) L. Zhao, J. Peng, Q. Huang, C. Li, M. Chen, Y. Sun, Q. Lin, L. Zhu, F. Li, *Adv. Funct. Mater.* **2013**, *23*, 363 – 371; b) X. Yang, X. Liu, Z. Liu, F. Pu, J. Ren, X. Qu, *Adv. Mater.* **2012**, *24*, 2890 – 2895; c) Y. Dai, H. Xiao, J. Liu, Q. Yuan, P. a. Ma, D. Yang, C. Li, Z. Cheng, Z. Hou, P. Yang, J. Lin, *J. Am. Chem. Soc.* **2013**, *135*, 18920 – 18929.
[6] a) W. Cao, Y. Gu, M. Meineck, H. Xu, *Chem. Asian J.* **2014**, *9*, 48 – 57; b) K. Tanabe, T. Asada, T. Ito, S.-i. Nishimoto, *Bioconjugate Chem.* **2012**, *23*, 1909 – 1914.
[7] Z. B. Starkewolf, L. Miyachi, J. Wong, T. Guo, *Chem. Commun.* **2013**, *49*, 2545 – 2547.
[8] P. Juzenas, W. Chen, Y.-P. Sun, M. A. N. Coelho, R. Generalov, N. Generalova, I. L. Christensen, *Adv. Drug Delivery Rev.* **2008**, *60*, 1600 – 1614.
[9] N. Ma, H. Xu, L. An, J. Li, Z. Sun, X. Zhang, *Langmuir* **2011**, *27*, 5874 – 5878.
[10] a) W. Fan, B. Shen, W. Bu, F. Chen, K. Zhao, S. Zhang, L. Zhou, W. Peng, Q. Xiao, H. Xing, J. Liu, D. Ni, Q. He, J. Shi, *J. Am. Chem. Soc.* **2013**, *135*, 6494 – 6503; b) W. Fan, B. Shen, W. Bu, X. Zheng, Q. He, Z. Cui, K. Zhao, S. Zhang, J. Shi, *Chem. Sci.* **2015**, *6*, 1747 – 1753.
[11] F. Yang, P. Chen, W. He, N. Gu, X. Zhang, K. Fang, Y. Zhang, J. Sun, J. Tong, *Small* **2010**, *6*, 1300 – 1305.
[12] a) S. Gai, C. Li, P. Yang, J. Lin, *Chem. Rev.* **2014**, *114*, 2343 – 2389; b) G. Chen, H. Qiu, P. N. Prasad, X. Chen, *Chem. Rev.* **2014**, *114*, 5161 – 5214; c) T. Yang, Y. Sun, Q. Liu, W. Feng, P. Yang, F. Li, *Biomaterials* **2012**, *33*, 3733 – 3742.
[13] a) J. Zhou, M. Yu, Y. Sun, X. Zhang, X. Zhu, Z. Wu, D. Wu, F. Li, *Biomaterials* **2011**, *32*, 1148 – 1156; b) Q. Liu, Y. Sun, C. Li, J. Zhou, C. Li, T. Yang, X. Zhang, T. Yi, D. Wu, F. Li, *ACS Nano* **2011**, *5*, 3146 – 3157.
[14] a) H. T. T. Duong, N. N. M. Adnan, N. Barraud, J. S. Basuki, S. K. Kutty, K. Jung, N. Kumar, T. P. Davis, C. Boyer, *J. Mater. Chem. B* **2014**, *2*, 5003 – 5011; b) P. G. Wang, M. Xian, X. Tang, X. Wu, Z. Wen, T. Cai, A. J. Janczuk, *Chem. Rev.* **2002**, *102*, 1091 – 1134; c) S. L. M. Shishido, A. B. Seabra, W. Loh, M. Ganzarolli de Oliveira, *Biomaterials* **2003**, *24*, 3543 – 3553.
[15] a) T. Cook, Z. Wang, S. Alber, K. Liu, S. C. Watkins, Y. Vodovotz, T. R. Billiar, D. Blumberg, *Cancer Res.* **2004**, *64*, 8015 – 8021; b) B. F. Jordan, P. Sonveaux, O. Feron, V. Gregoire, N. Beghein, C. Dessy, B. Gallez, *Int. J. Cancer* **2004**, *109*, 768 – 773; c) M. De Ridder, D. Verellen, V. Verovski, G. Storme, *Nitric Oxide* **2008**, *12*, 164 – 169.
[16] a) X. F. Zhang, S. Mansouri, D. A. Mbeh, L. H. Yahia, E. Sacher, T. Veres, *Langmuir* **2012**, *28*, 12879 – 12885; b) A. Lutzke, A. P. Jurado, B. H. Neufelda, M. M. Reynolds, *J. Mater. Chem. B* **2014**, *2*, 7449 – 7458; c) J. Xu, F. Zeng, H. Wu, C. Hu, C. Yu, S. Wu, *Small* **2014**, *10*, 3750 – 3760.
[17] J. Sun, X. Zhang, M. Broderick, H. Fein, *Sensors* **2003**, *3*, 276 – 284.
[18] J. Takahashi, M. Misawa, *Radiat. Phys. Chem.* **2009**, *78*, 889 – 898.
[19] N. M. Idris, M. K. Gnanasammandhan, J. Zhang, P. C. Ho, R. Mahendran, Y. Zhang, *Nat. Med.* **2012**, *18*, 1580 – 1585.
[20] Q. Xiao, X. Zheng, W. Bu, W. Ge, S. Zhang, F. Chen, H. Xing, Q. Ren, W. Fan, K. Zhao, Y. Hua, J. Shi, *J. Am. Chem. Soc.* **2013**, *135*, 13041 – 13048.

Received: May 19, 2015
Revised: June 21, 2015
Published online: July 23, 2015

